Synthesis, Characterization and Photocatalytic Application of Mn Doped ZnO ($Mn_xZn_{1-x}O$) Nanoparticles

S. Chauhan[*], M.S. Chauhan[*], R. Kumar[*], D. Rana[*] and A. Umar[**]
[*]Department of Chemistry, H.P. University, Shimla 171005 (India), scschauhan19@gmail.com
[**]Department of Chemistry, Faculty of Sciences and Arts and Promising Centre for Sensors and Electronic Devices (PCSED), Najran University, Najran-11001, Kingdom of Saudi Arabia

ABSTRACT

This work presents the characterization of Mn-doped ZnO nanomaterials ($Mn_xZn_{1-x}O$; x = 0.01, 0.02, 0.05, 0.1 and 0.2) fabricated using simple solution process in terms of FESEM, EDS, XRD and UV-visible spectroscopy. The presence of dopant, Mn^{2+} is observed to have significantly influenced the morphology of the ZnO nanorods; ZnO nanorods undergo transformation to nanoparticles in the presence of Mn^{2+}. The material has been subjected to its photocatalytic activity by performing the degradation of aqueous solution of RhB dye solution of ~ 10 ppm under UV light. 10% Mn doped ZnO showed superior photocatalytic activity as compared to other synthesized samples. This improvement in the photocatlytic activity of the Mn doped ZnO nanoparticles toward photodegradation of Rhodamine B (RhB) is suggested to be due to the inhibition of recombination of charge carriers resulting from the increase in surface area and crystallinity which is in accordance with the FESEM results.

Keywords: Mn-doped ZnO, FESEM, XRD, UV-visible, Raman spectroscopy

1 INTRODUCTION

Zinc oxide (ZnO) is an mportant member of II-VI group semiconductors. In addition to its direct and wide band gap of 3.37 eV, a large excitation binding energy of 60 meV [1-3], ZnO is known to exhibit piezoelectric and pyroelectric properties, and has the key advantage of being bio-compatible [3-5]. These properties have a great deal of bearing on ZnO as a material for potential applications in various emerging areas of nanotechnology [1-12]. Furthermore, the introduction of transition metal ion as impurity has evoked keen interest to investigate ZnO-based nanoscale materials for their potential use in various fields [13-15].

In the present work we report synthesis of Mn-doped ZnO nanomaterials using a simple aqueous solution method under ambient conditions using the dopant, Mn^{2+} in different concentrations and the host precursor, ZnO synthesized using the fixed concentration of the raw materials. The addition of Mn^{2+} has been found to produce a significant change in the morphology of pure ZnO nanostructure (nanorod) that has a strong bearing on the photocatalytic properties of Mn-doped ZnO nanoparticles.

2 EXPERIMENTAL

The reagents, Zinc nitrate hexahydrate, $Zn(NO_3)_2.6H_2O$ and manganese chloride dehydrate, $MnCl_2.2H_2O$ were purchased from Sigma–Aldrich. Sodium hydroxide, NaOH of AR grade was obtained from E. Merck (India) and Rhodamine B (RhB) was purchased from M.P. Biomedicals. All the reagents were used as received without further purification.

2.1 Synthesis of Undoped and Mn Doped ZnO Nanomaterials

Pure ZnO nanorods were synthesized using simple solution approach at low temperature ~60^{o}C. In a typical synthesis process: 100 ml aqueous solution of 0.01 M NaOH was carefully added to 100 ml aqueous solution of 0.01 M $Zn(NO_3)_2.6H_2O$ under continuous stirring. Few extra drops of NaOH were added to maintain the pH of the resulting solution as 12 before subjecting the solution to refluxing for 6 h at 60 ^{o}C. Afterwards, the reaction mixture was allowed to stand still overnight. The white precipitates thus obtained were washed with deionized water for 2-3 times. Finally, after washing the precipitates with methanol and ethanol, they were dried in hot air oven for 6-8 hr.

The synthesis of Mn doped ZnO nanomaterials, for instance, in case of 1% Mn doped ZnO, 100 ml aqueous solution of 0.001 M $MnCl_2.2H_2O$ was added first drop-wise into 100 ml of 0.01M $Zn(NO_3)_2.6H_2O$ under stirring condition. This was followed by the addition of 100 ml of 0.01M NaOH. Similar synthesis procedure was performed to incorporate different levels of Mn dopant (2, 5, 10 and 20%) in ZnO nanorods by varying the relative concentration of Mn accordingly.

2.2 Characterizations

The morphological characterization of as synthesized ZnO and Mn doped ZnO nanomaterials were done by field emission scanning electron microscopy (FESEM) JEOL–JSM–7600F. Elemental analysis was conducted by using energy dispersive spectroscopy attached with FESEM. The structural analysis of the samples were carried out by X-ray diffractometer (XRD; PANalytical X'Pert PRO) measured with Cu- Kα radiations (λ = 1.54178 Å) in the range of 10–70◦ with scan speed of 8°/min. To examine the optical properties of as synthesized Mn doped ZnO nanoparticles room-temperature UV–Vis spectrum (Carry 100 Bio UV–Vis spectrophotometer) was recorded.

2.3 Photocatalytic Degradation of Rhodamine B (RhB) Using Mn Doped ZnO Nanoparticles

Photocatalytic activity of as-synthesized 1, 2, 5, 10 and 20 % Mn doped ZnO nanoparticles were studied for their degradation efficiency of Rhodamine B (RhB) under UV irradiation at different time intervals. The degradation of RhB was monitored by measuring the absorbance at regular time intervals using UV-Visible spectrophotometer Cary 100 Bio at $\lambda = 553$ nm. The degradation reaction was performed in a 250 ml beaker, which contain 10 ppm aqueous solution of RhB and Mn doped ZnO nanomaterials. Irradiation was done with 125 W Mercury lamps. The rate of degradation for the decomposition of RhB was estimated by evaluating the change in absorbance at $\lambda_{\mu\alpha\xi} = 553$ nm and the degradation of the RhB dye was calculated using the relation [11]

$$\eta = \frac{A_o - A}{A_o}$$

where A_o is the absorbance of aqueous RhB dye solution prior to the addition of photocatalyst and UV exposure and A is the absorbance of RhB in reaction suspensions with the photocatalyst following UV exposure for definite time.

3 RESULTS AND DISCUSSION

The morphology and structure of pure ZnO and $Zn_{1-x}Mn_xO$ (x = 0.01, 0.02, 0.05, 0.10 and 0.20) characterized by FESEM confirm the formation of ZnO nanorods with average diameter of 100nm and length of 700 nm (Fig. 1). On the addition of Mn^{+2} ions the rod like morphology of pure ZnO gets completely transformed into particles even at a very small fraction i.e. 1% of Mn^{+2} ions. Such morphological transformations have also been observed by Wang et al. [16] who have reported the transformation of nanorods like morphology of ZnO into noparticles on the addition of Cu^{+2} ions. Yang et al. [17] have observed the similar kind morphological transformation by Cr doping. Yang et al. [18] have discussed the change in morphology of ZnO nanoparticles to tetrapods and nanorods.

XRD results of as-synthesized nanomaterials have been summarized in Fig. 2. It can be seen that all the diffraction peaks at scattering angle, 2θ: 31.43, 34.12, 35.91, 47.26, 56.29, 62.54, 67.64, and 68.82 correspond to hexagonal wurtzite structure of ZnO (JCPDS 36-1451). Also, sharp and intense diffraction peaks can be attributed to highly crystalline nature of synthesized Mn doped ZnO nanoparicles. No diffraction peak corresponding to the MnO_2 is observed in the XRD spectra of samples upto 10% doping level. Hence it is inferred that as synthesized particles are single phase upto 10% Mn. This might be due to the successful substitution of Zn^{2+} (0.74Å) by Mn^{2+} (0.66Å). However, appearance of a small diffraction peak at 41.98° in case of 20% Mn doped ZnO correlates to (200) plane of MnO (JCPDS 78- 0661). Hence a new phase corresponding to MnO_2 appears to exist above 10 % of the Mn^{2+} due to the oxide form of un-reacted dopant metal ion.

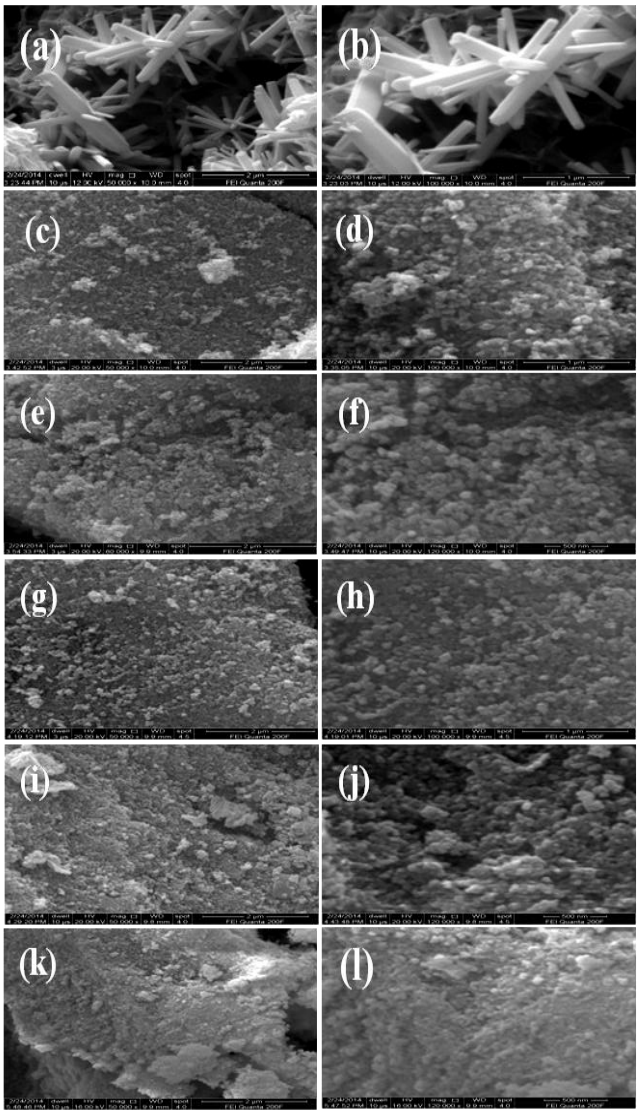

Figure 1: (a, b) Low and (c-l) high-magnification FESEM images, of as-synthesized Mn doped ZnO nanoparticles.

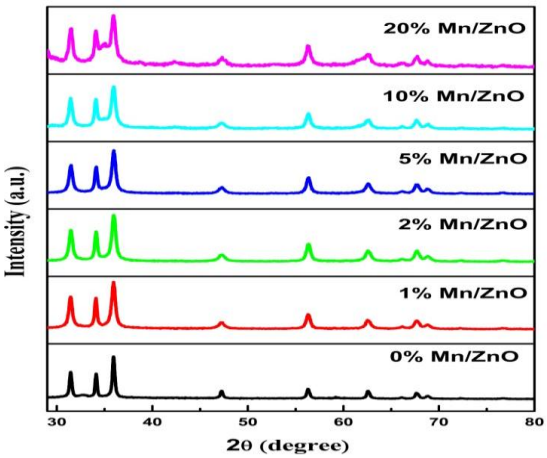

Figure 2: XRD pattern of of as-synthesized Mn doped ZnO nanoparticles

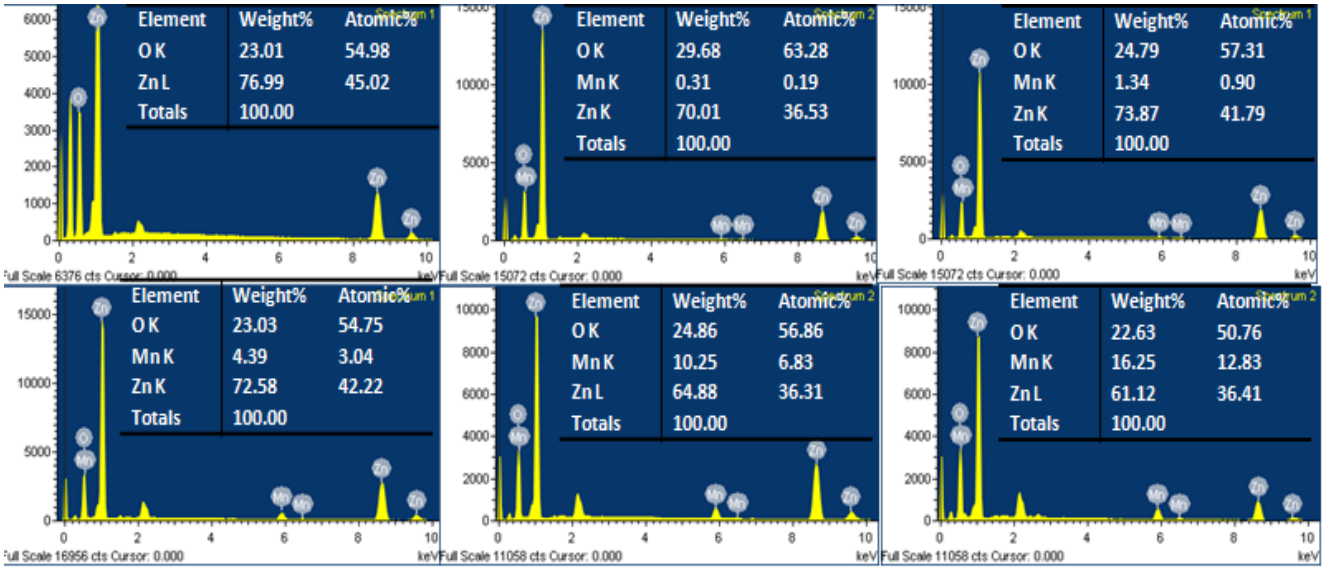

Figure 3: EDS pattern of of as-synthesized Mn doped ZnO nanoparticles.

The compositions and purity of Mn doped ZnO nanoparticles determined by EDX measurements have been shown in Fig. 3. It is clear from the spectra that as synthesized Mn doped ZnO are composed of only Zn, Mn, and O elements. The estimated % age of impurity atom in $Mn_xZn_{1-x}O$ (x=0.01, 0.02, 0.05, 0.1 and 0.2) nanoparticles are as follows: 0.19, 0.90, 3.04, 4.87 and 14.56. Hence we find that as synthesized $Zn_{1-x}Mn_xO$ nanoparticles are pure with homogenous distribution of Mn^{+2} ions impurity through the surface of nanorods of ZnO.

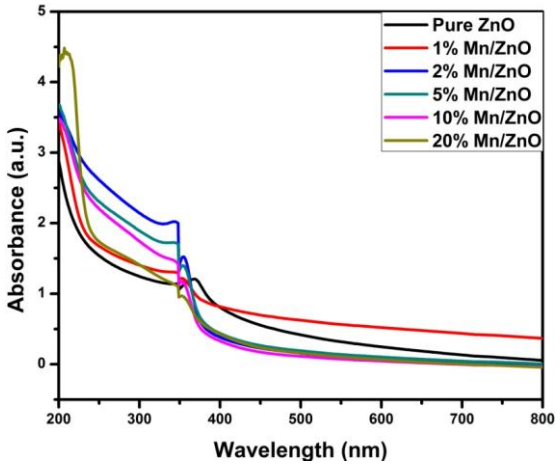

Figure 4: UV-Visible spectra of as-synthesized pure ZnO and 1, 2, 5, 10 and 20% Mn doped ZnO nanoparticles.

From (Fig. 4) we find the appearance of a sharp absorption band at 376 nm, which corresponds to the calculated band gap of ZnO as, E_g = 3.29 eV. However on increasing the concentration of Mn a gradual decrease in the absorption intensity initially up to 10 % Mn is found to be increased abruptly at 20 % Mn. This can be explained on the basis that at low doping concentration of Mn^{2+} (1, 2, 5 and 10%) there is almost substitutional doping of Zn^{2+} ions by Mn^{2+} in the ZnO matrix. Above 10 % concentration of dopant Mn^{2+}, however the dopant occupies interstitials sites in ZnO matrix, because at 20% Mn doped ZnO sample, in particular, we find two optical absorption bands appearing at 208 and 352 nm. These correspond to MnO_2 and $Mn_xZn_{1-x}O$ respectively. These results are in good agreement with XRD data. A decrease in the absorption band from 376 nm for pure ZnO sample to 353, 355, 354, 353 and 352 nm respectively for 1, 2, 5, 10 and 20% Mn doped ZnO indicate the occurrence of blue shift on account of the Mn^{2+} dopant ions and is a clear indication of increase in band gap value of ZnO with increasing impurity ion conc. Thus explaining the transformation of ZnO morphology from nanorods to the nanoparticles in the presence of Mn^{2+} as dopant.

3.1 Photocatalytic Properties of Pure and Mn Doped ZnO Nanoparticles.

The photocatalytic results of the present studies have been presented in Fig. 5. Fig. 5 (a) shows the variation of UV intensity of RhB with respect to 10% Mn doped ZnO nanoparticles. It has been observed that there is gradual decrease in absorption maxima of RhB dye and almost complete degradation is achieved after ~ 70 min of UV exposure. Fig. 5 (b and c) represent the variation of A/Ao and percentage photodegradation as a function of time for all the synthesized samples. It is clear from the Fig. 5 (c) that complete degradation of RhB (10ppm) has occurred using 0.05 g of 10% Mn doped ZnO sample while only 45% degradation of RhB takes place in pure ZnO nanorods in the same set of conditions.

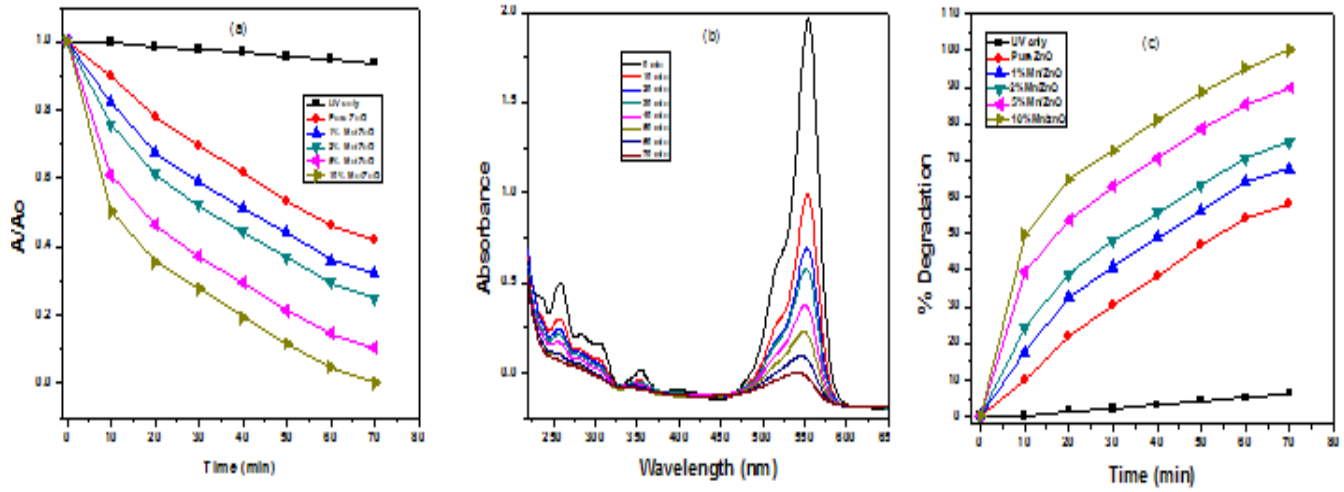

Figure 5: (a) UV-Visible spectra of RhB (10 ppm) dye containing 0.05g of 10% Mn doped ZnO nanoparticles at different intervals. (b) Plot for extent of decomposition (A/A_o) of RhB dye with respect to time intervals, (c) plot for % degradation of RhB dye versus time of irradiation.

This can be seen as corroborating the consequences of morphological changes and crystallinity of the as-synthesized samples from nanorods to nanoparticles. The increase in surface area and crystallinity on account of decrease in the size are expected to increase the number of active sites and the separation of photogenerated charges. This appears to justify the observed higher photocatalytic activity of 10% Mn^{2+} doped ZnO nanostructured sample in comparison to the pure ZnO.

4 CONCLUSIONS

In conclusion, we find that there is a good deal of improvement with regards to the photocatalytic properties of ZnO nanomaterials when doped with Mn^{2+} transition metal ion, which is due primarily to the change in the morphology of the sample as well as the reduction in the size of ZnO. In particular, however, it was interesting to note the appearance of a new phase corresponding to MnO_2 above 10 % Mn^{2+}. Hence we find that as - synthesized $Zn_{1-x}Mn_xO$ nanoparticles are pure with homogenous distribution of Mn^{+2} ions impurity below 10 % Mn^{2+}.

Acknowledgement

RK thanks CSIR, New Delhi for the award of SRF.

REFERENCES

[1] L. Jianwei, M. Shouzhi, L. Xinjuan, Z. Zhaofen and Q. S. Chang, Chem. Rev., 112, 2822, 2012.
[2] W.W. Li, W.L. Yu, Y.J. Yu, C.B. Jing, J.Y. Zhu, M. Zhu, Z.G. Hu, X.D. Tang and J.H. Chu, J. Phys. Chem. C, 114, 11951, 2010.
[3] Y. Wang, T. Hou, T. Sheng, S.-T. Lee and Y. Lee, J. Phys. Chem. C, 115, 7706, 2011.
[4] M.Q. Israr, J.R. Sadaf, L.L Yang, O. Nur, M. Willander, J. Palisaitis and P.O.A. Persson, Appl. Phys. Lett., 95, 073114, 2009.
[5] Z.L. Wang, ACS Nano., 2, 1987, 2008.
[6] M. Wang, G.T. Fei, and L.D. Zhang, Nanoscale Res. Lett., 5, 1800, 2010.
[7] J. G. Yu and X.X. Yu, Environ. Sci. Technol., 42, 4902, 2008.
[8] F. Wang, Y. Han, C.S. Lim, Y.F. Lu, J. Wang, J. Xu, H. Chen, C. Zhang, M. Hong and X. Liu, Nature, 463, 1061, 2010.
[9] A. Umar, M.S. Chauhan, S. Chauhan, R. Kumar, G. Kumar, S.A. Al-Sayari, S.W. Hwang and A. Al-Hajry, J. Colloid Interf. Sci., 363, 521, 2011.
[10] A. Umar, M.S. Chauhan, S. Chauhan, R. Kumar, P. Sharma, K.J. Tomar, R. wahab, A. Al-Hajry and D.S. Rana. J. Biomed. Nanotech. 9, 1, 2013.
[11] R. Kumar, D. Rana, A. Umar, P. Sharma, S. Chauhan and M.S. Chauhan Sensor Letters,12, 1, 2014.
[12] R. Kumar, D. Rana, A. Umar, P. Sharma, S. Chauhan and M.S. Chauhan, Talanta, 137, 204, 2015.
[13] B. Panigrahy, M. Aslam and D. Bahadur, J. Phys. Chem. C,114, 11758, 2010.
[14] K. Sato and H. Katayama-Yoshida, Jpn. J. Appl. Phys, 39, L555, 2000.
[15] R. Liu, L. Shi and B. Zou, Appl. Mater. Interf., 6, 10353, 2014.
[16] H.B. Wang, H.C. Zhang, F.J. Yang, J.X. Duan, C.P. Yang, H.S. Gu, M.J. Zhou, Q. Li and Y. Jiang, J. Nanosci. Nanotech., 9, 3308, 2009.
[17] J.H. Yang and P.H. Holloway, Nanotechnology, 17, 973, 2006.
[18] Y. Yang, Y. Jin, H. He, Q. Wang, Y.H. Lu and Z. Ye, J. Am. Chem. Soc., 132, 13381, 2010.